

Information theory and player deck choice in online Collectable Card Games

Mathew Zuparic,¹ Duy Khuu,² and Tzachi Zach³

¹Defence Science and Technology Group, Canberra, ACT 2600, Australia

²Australian National University, Canberra ACT 2601 Australia

³Ohio State University, Columbus OH 43210 United States

Using three years of player data of the online Collectible Card Game *Hearthstone*, we perform an in-depth analysis of the evolution of the game’s online landscape over the period 2016–2019. Specifically, by considering the frequencies that deck archetypes are played, and their corresponding win-rates, we are able to provide narratives of the system-wide changes that were made over time, and how players reacted to those changes via their choices regarding deck construction and tactics. Applying the deck frequencies to analyse the system’s Shannon entropy, we characterise the salient features of player deck choice over time. Paying particular attention to how system entropy is affected during periods of both small and large-scale change, we are able to demonstrate the effects of increased player experimentation before clear viable decks and tactics emerge. Furthermore, guided by the concept of local active information storage, we construct conditional probabilities that particular decks are chosen, given previous deck frequencies and win-rates. Importantly, these conditional probabilities can be interpreted to simulate understandable player behaviour. Then comparing the Shannon entropy with the expectation value of the local active information storage over all past and current deck choices and win-rates, we are able to test the explain-ability of current player choice based on previous player decision-making.

I. INTRODUCTION

Over the past number of decades Collectible Card Games (CCGs) have been steadily emerging as a pervasive form of play amongst a wide age bracket. In particular, the appearance of *Magic: the Gathering* in 1993 managed to capture enough popularity that by its 25th-year anniversary, approximately 20 billion physical cards had been printed [1]. Of course the landscape that CCGs operate in has expanded considerably since those early days — from table-top sessions involving physical cards and relatively few players, to online experiences such as those offered by *Hearthstone*, where servers accommodate over one hundred million players world-wide.

Player choice in most adversarial games (*Chess*, *Go*, etc.) is limited to the in-game experience. In these situations, the distinguishing factor of who wins is usually the more experienced player, who will (on average) make better choices over the course of a match. CCGs such as *Magic: the Gathering*, *Yu-Gi-Oh!* and *Hearthstone* possess the distinguishing feature of requiring players construct their specific deck of cards *before* they engage other players in a tactical match. Decks consist of a limited number of cards (approximately thirty) from a potential pool of thousands. The act of constructing a deck is arguably the most meaningful choice a CCG player will make, as it usually determines the tactics that will be pursued during a match, with popular decks (also referred to as *archetypes*) emerging over time. Indeed, players engaging in deck construction in order to maximise their chances of winning is an abstraction of the project-portfolio optimisation activities commonly occurring in the finance [2] and defence [3] sectors.

In an online setting where decks are constructed and games are played in a shared environment, CCGs can be thought of to exist within a substantial system. In Figure 1 we present an abstraction of this system, divided into three layers; *tactical*, *meta* and *authority*. The tactical layer is where deck-construction and gameplay occurs. For any competitive online CCG, the layer above the tactical — the meta — can

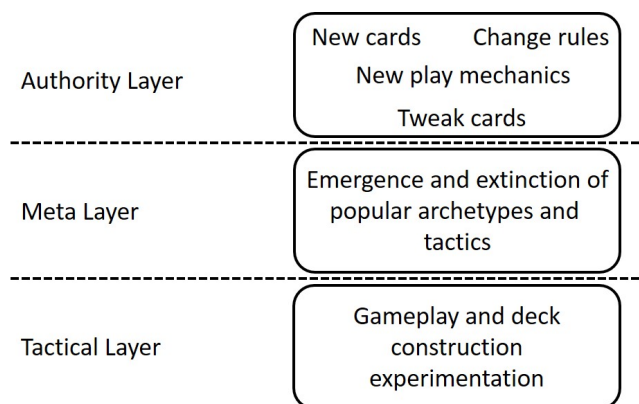


FIG. 1: Abstraction of the online CCG *landscape* consisting of three separate layers: *tactical*, *meta* and *authority*.

be articulated as the emergence of popular and viable deck archetypes and corresponding tactics over time, as players experiment with different play-styles. As explained by Carter *et al.* [4], though the meta is *peripheral* to the rules and mechanics of the game itself, it nonetheless provides an understanding to what players will experience in an online competitive setting. The top layer in Figure 1 — authority — is the remit of the publisher of the CCG. At various times, the authority layer will initiate changes into the tactical layer of the CCG, either by changing cards, adding new cards or changing rules and/or play mechanics which inevitably affect player deck archetype choices.

A. Past research

Due to the underlying difficulty involved in deck construction, the majority of past research in CCGs has been focused between the tactical and meta layer — primarily on the discovery of optimal decks or determining the best moves to

make during a given instance of the game. Illustrating this, García-Sánchez *et al.* [5] developed an evolutionary algorithm to continuously evolve an initial deck and showed a noticeable improvement in win-rates against the majority of other deck archetypes after 50 generations. In 2014 Bursztein [6] was able to use data from 50,000 recorded games to predict which cards an opponent would likely play on a given turn, boasting over a 95% accuracy for its prediction after the second card is played. Remarkably, the publishers of the CCG requested that Bursztein not publicly release the resulting algorithm as it was demonstrably game breaking. Stiegler *et al.* [7] applied a utility system to automatically construct decks which considered a number of metrics relating to gameplay (cost effectiveness, card synergies, *etc.*), as well as considering on how popular chosen cards are in the current meta. The authors found that their algorithm was able to complete deck skeletons into currently popular archetypes. Fontaine *et al.* [8] explored the use of a *quality-diversity* algorithm, where both novelty and performance were incentivised in an attempt to imitate player decision-making and determine a set of popular decks for each class. Once these decks were established a selection of popular cards were negatively affected — *nerfed* — to reduce their viability and the algorithm was run again to reveal counter-intuitive results. Specifically, various popular cards whose *resource cost* was increased were included more frequently when constructing popular archetypes — suggesting that even an objectively negative change may have a positive impact on the perception of a card’s viability. Correspondingly Bhatt *et al.* [9] found that decks constructed by their algorithms possessed some degree of generality — performing well against decks not in the current meta. A less-focused-on topic is the meta layer of CCGs. One recent example is de Mesentier Silva *et al.* [10] who applied an evolutionary algorithm in an attempt to understand the impacts on the meta that are brought about by improving and/or worsening various cards. The authors noted that while it was possible to balance the meta after initiating change, too much change led to disruptive effects which were difficult to resolve.

B. Intent of this work

In this work we focus our attention on the CCG system itself as presented in Figure 1 — to the best of our knowledge a topic not actively studied thus far. *Essentially — at a system-wide level — we seek to analyse and understand how changes enacted to the CCG by the publishers influence player decision-making.* Specifically, we are interested in characterising the salient features of the game’s online landscape and demonstrating how small and large-scale changes into the tactical layer — initiated from the authority layer — influence the evolution of the CCG’s meta, and by extension the decisions players make in deck construction. To enable this analysis we use three years of gameplay data from the CCG *Hearthstone*, considering both the frequencies that deck archetypes are played, and their corresponding win-rates over the 2016–2019 period. To understand the effects that changes enacted by the publishers have on the *Hearthstone* system, we

focus on various information-theoretic measures as they are a method to quantify the amount of surprise, randomness and complexity in an entire system. Analysing the *Hearthstone* meta through the lens of information entropy, we understand and characterise the evolution of complexity and uncertainty in the meta at any given time — paying particular attention to how players respond and adapt to changes initiated by the publishers. Furthermore, by considering the information storage exhibited within *Hearthstone*’s meta, we are able to estimate how much previous player decision-making explains the underlying structure seen in the current state of the CCG.

C. Common tactical elements of Collectible Card Games

During a match, two adversaries take turns selecting and *playing* cards from their *hand*. At the start of each turn a specific amount of cards are randomly dealt to the player’s hand, drawn from the deck which has been constructed by the player before the match. During a player’s turn cards are *activated* or played by spending a predefined amount of in-game resource which is replenished at the end of the player’s turn. Cards that have been activated are then sent to the player’s *discard-pile* and are typically out of play for the remainder of the match. The ultimate goal for each player is to reduce their adversary’s in-game *health* to zero, triggering a *win*. Though we focus on *Hearthstone* for the majority of this work, we remark that many of the elements discussed in this section apply to the majority of CCGs.

At the very heart of CCGs are the cards themselves, which generally fall under two categories: *minions* and *spells*. When activated, minion cards offer the player one or more controllable characters on the *playing-field*, acting as a tangible line of defence between the player, and the adversary. Three common properties of all minion cards include: *resource cost*, the in-game resource required to activate the minion; *strength*, the amount of damage the minion can do to the adversary and/or their minions; and *health*, the amount of damage the minion can receive until they are removed from the playing-field. Spell or *effects* cards range from single-use damage-dealing cards, to cards which perform sustained effects over multiple turns. Specific to *Hearthstone* [6, 10] are *weapon* cards, equippable by the player, *secret* cards, similar to spells but triggered once specific conditions are met, and *hero* cards, replacing the player’s in-game avatar and changing their properties. For more information specifically regarding *Hearthstone* we refer the reader to [11] and references therein.

Generally, cards in all CCGs come with many different properties in addition to the listed common properties, and the varied *synergies* among these properties directly affect the choices players make when constructing their deck. For instance, the activation of many *high value* cards may require complex conditions to be satisfied which are only made possible (or at least more probable) if certain other cards are present in the player’s deck.

D. Deck archetypes and character classes

One of the most important common elements across CCGs are the deck archetypes. Fundamentally, decks *generally* fit into three overarching archetypes, and understanding which decks fall under which type (or combination of types) enables a rudimentary understanding of how that deck will generally function against other decks. The overarching deck types are:

- *Aggro* decks rely on aggressive tactics to achieve victory. These decks typically focus on low cost cards with the intent to overwhelm the adversary in the early stages of the match. Typically, aggro players that cannot maintain significant tempo in the early-to-mid stages of the match find themselves losing.
- *Control* decks rely on relatively high-cost and high-value cards to win in the later stages of a game. The moniker *control* comes from the deck's necessity in the early-to-mid game to counter a variety of play-styles, thus granting player the time needed to initiate the intended late-game finishing tactics.
- *Combo* decks generally rely on cards which contain synergies, with the intent to knock out the opponent by playing a number of cards in conjunction with each other to generate devastating effects. Much like control decks, combo decks must have some form of counter for aggressive early-game play-styles, but mirroring aggro decks, they also rely on knocking out control decks before their high-cost high-value cards are activated.

In addition to choice of archetype, specific to *Hearthstone* in the 2016–2019 period players must choose one of nine character classes: *Druid*, *Hunter*, *Mage*, *Paladin*, *Priest*, *Rogue*, *Shaman*, *Warlock* and *Warrior*. Besides characters providing unique abilities, players gain access to character specific cards. These character cards mean that some characters generally favour specific deck archetypes — for instance the *Mage's* considerable range of spell cards, and their ability to deal with a large number of adversary minions, means that many of the *Mage*-based decks gravitate towards variants of the *control* archetype.

As explained in [10], deck construction choices and play-styles become popular and emerge in the meta for a host of reasons, either because the particular style ensures the highest probability of win, or provide robust counters to other popular play-styles. Additionally, two deck-lists considered part of the same archetype may not be identical due to play-style preferences or differing perceptions on the viability and strength of particular cards. Though, as articulated in [8], players can be motivated by less tangible reasons, including simply finding certain combinations of cards particularly fun to play. A *Hearthstone* specific example of this is the card *Marin the Fox*, which when summoned creates a treasure chest that, once destroyed, grants the player with one of a number of extraordinarily powerful cards. It was recognised that successful implementation of this tactic was especially challenging, and posed many risks for the player as a number of archetypes

possessed abilities which would allow the opponent to destroy the chest and steal the resulting powerful cards for themselves. Nevertheless, despite these considerable risks and challenges this card did appear in a number of decks due to how satisfying to play the chest's rewards were once obtained. Thus the meta is influenced by a whole host of player choices made in deck construction, their behaviour during play and their motivations (to win, enjoyment, *etc.*)

E. Information-theoretic measures

Reiterating, our main method of studying and gaining insights from the *Hearthstone* meta will be by applying information-theoretic measures to approximately three years of archetype frequency and win-rate data. Information-theoretic entropy measures are a method to quantify the amount of *surprise* or *randomness* in an entire system [12]. That is, *how likely are particular outcomes assured?* In a system such as *Hearthstone's* meta, the relevant questions are centred around the number of deck archetypes currently active, and how balanced the outcomes are over any given time period. Specifically, *Shannon information entropy* measures the uncertainty (or surprise) within a system consisting of a single set of elements — in our case these are the time-ordered deck frequencies which define the evolution of the meta. Furthermore, associated with information entropy is the concept of system *criticality* [13], sometimes referred to as the *edge of chaos* [14]. In mathematical [15, 16], physical [17], biological [18, 19], computational [20, 21], and financial [22] systems, amongst others, criticality refers to the system being able to respond and adapt to a rapidly changing environment. Intuitively, it can be viewed as a dynamical system cycling through periods of relatively low and high entropy, spending the majority of its time in intermediate entropy values. For a gentle introduction into this topic we refer the reader to [23, 24].

In order to gain additional insights from the meta, we apply the concepts of distributed information storage [25], closely related to information transfer [26]. The formulation of a systematic explanation of how information is stored, processed and transferred in distributed systems arguably began in earnest at the start of the 21st century with Schreiber's [27] landmark work on *information transfer entropy*, mathematically defining how information is transferred between distinct processes in a distributed system. Information transfer has since been applied to great effect in a wide range of applications, including neuroscience [28], multi-agent dynamics [29], and social media [30].

A decade after Schreiber's result, Lizier *et al.* [31] introduced the concept of *local active information storage* (LAIS). Intuitively, LAIS can be applied to detect how much of the past information within the distributed system contributes to its current state. Ideas stemming from this concept have been applied to further understand how information storage properties affect network structure in biological and artificial networks [32], further distinguish the dynamics displayed in cellular automata [31], and characterise normal and diseased

states in cardiovascular and cerebrovascular regulation [33].

Particularly relevant to this work are the following studies — using information storage to determine the amount of information in a system’s past used in generating its next state. Wibrál *et al.* [34] measured the local time and space voltage neurologically generated by stimulating the visual cortex of an anaesthetised cat. The spatio-temporal structure of the corresponding LAIS data was then used to understand how the onset of visual stimulus led to spatio-temporal surprise (or misinformation) about the proceeding visual outcomes. Wang *et al.* [35] explored collective memory/storage via an information-theoretic characterisation of cascades within the dynamics of simulated swarms. Using the interpretation that the LAIS of a system component characterises the amount of past data used to predict the component’s next state, the authors calculated the system-wide *active information storage* (AIS) by taking the expectation value over all component states at any time period. They verified a long-held conjecture that information, used for computation by the swarm, cascaded via waves rippling through the swarm, and found that higher values of storage generally correlate with greater dynamic coordination. Cliff *et al.* [36] explored the AIS within a multi-agent team by analysing implicit team interactions. Specifically, the authors noted that when an agent’s AIS values were high, this corresponded to its movements being predictable — *i.e.* correlating highly with the previous system state(s). In this work we extend these results by applying information storage to test how much previous player decision-making — *i.e.* frequency that archetypes are played — explains the underlying structure seen in *Hearthstone’s* meta.

F. Mathematical preliminaries

Though Shannon entropy and criticality may be relatively ubiquitous concepts, we shall devote this section to introducing readers to the underlying mathematics behind LAIS. Beginning with a given variable set $\{X^T, X^{T-1}, \dots, X^{T-K}\}$ of $K + 1$ time-ordered states, the LAIS of the state X^T at time T , based on its past K states, is given by

$$a_K(X^T) = \log_2 \frac{\mathcal{P}(X^T | X^{T-1}, \dots, X^{T-K})}{\mathcal{P}(X^T)}. \quad (1)$$

In previous studies the values of the LAIS in Eq.(1) were interpreted as follows: positive values implied that the past states of the variable provide information and positively correlate with the current state. Conversely, negative values of LAIS indicate that the variable’s past history does not correlate with its next state — synonymous with surprise. With this interpretation, we can see that the local past history of the variable correlates with its current value only if the conditional probability $\mathcal{P}(X^T | X^{T-1}, \dots, X^{T-K})$ in Eq.(1) is greater than the marginal probability $\mathcal{P}(X^T)$ of the event occurring. Furthermore the expectation value of the LAIS, simply known as the

AIS

$$\begin{aligned} A_K^T &= \langle a_K(X^T) \rangle \\ &= \left[\prod_{n=1}^K \sum_{X^{T-n} \in \mathcal{X}^{T-n}} \right] \mathcal{P}(X^T, X^{T-1}, \dots, X^{T-K}) a_K(X^T) \end{aligned} \quad (2)$$

can be understood as a characterisation of the *explain-ability* [31] of the information in the system. That is, given a complete set of conditional and marginal probabilities which characterise a system, the AIS — when compared to the corresponding Shannon entropy — gives the amount of information in the current system that *is* explainable by the results of the previous time step(s).

To further understand this concept of explain-ability, related to AIS is the concept of the *entropy rate* \mathcal{E}_K^T , given by

$$\mathcal{E}_K^T = -\langle \log_2 \mathcal{P}(X^T | X^{T-1}, \dots, X^{T-K}) \rangle. \quad (3)$$

Complementary to AIS, the entropy rate — when compared to the corresponding Shannon entropy — characterises the amount of information in the current system which *is not* explainable by the results of the previous time step(s).

Importantly, following the work of Crutchfield and Feldman [37] and Lizier *et al.* [31] the contrast between what is explainable and what isn’t in the system is made clear by the following duality relation between Shannon entropy of the current state — labeled $\mathcal{H}(\mathcal{X}^T)$ — AIS and the entropy rate via

$$\mathcal{H}(\mathcal{X}^T) = A_K^T + \mathcal{E}_K^T. \quad (4)$$

Thus using Eq.(4), we can see that the percentage of information within the system which is explainable by past results is given by $A_K^T / \mathcal{H}(\mathcal{X}^T)$, with the remaining $\mathcal{E}_K^T / \mathcal{H}(\mathcal{X}^T)$ being the current system state not explained by past results.

G. Outline of the paper

In the next section we detail the *Vicious Syndicate* website which is the source of our *Hearthstone* archetype frequency and win-rate data. Using this data, we then construct sample timelines of some deck archetypes, demonstrating the dynamic evolution of the meta over time. We then look at this data through the lens of Shannon entropy, paying special attention to its behaviour around periods of small and large scale change initiated by the publishers. In Section III we mathematically construct conditional probabilities which simulate relatively simple, but nonetheless understandable, behaviour of players choosing specific decks, given past archetype choices and win-rates. These conditional probabilities are then used to define the system-wide AIS values per time period, ultimately applying Eq.(4) in an attempt to understand how much of *Hearthstone’s* past state of deck frequencies and win-rates contributes to its current state. In Section IV we offer further discussion and detail potential future work.

II. DATA EXPLANATION AND EXPLORATION

A. Data collection and preparation: Vicious Syndicate

Vicious Syndicate has been collecting *Hearthstone* game data systematically since May 2016. The data was used to produce weekly *Data Reaper Reports* about the state of the *Hearthstone* meta-game [38] — with short breaks generally occurring near the release of new content by *Hearthstone*'s publishers. To contribute game data, players are asked to install a small plugin that records their game play. That data is transmitted to the *Vicious Syndicate* team to be processed.

During any week between 2000 to 5000 players contributed game data, with tens of thousands of games being processed to produce reports. Specific numbers of contributing players and processed games can be found in each of the corresponding *Data Reaper Reports* [38]. Only games of rank 15 and above are included for reporting purposes, which excludes the bottom 40% of players. As explained in [39], in an attempt to provide an unbiased picture of the meta over time, only opponent decks are included for deck frequency reporting, so as to avoid potential over-representation of decks favoured by players who contribute data. Deck identification algorithms are applied to identify archetypes based on the cards played during a match. Importantly, though not every game provides a definitive identification, current algorithms achieve a very high success rate ($> 95\%$) when archetypes are identified. Additionally, win-rates are evaluated by taking the average of particular deck match-ups from the player perspective (those who contribute data) and the opponent perspective. If a sufficient number of games are played, differences in win-rates depending on perspectives suggest a mis-match in proficiency at playing these decks. In an attempt to correct these discrepancies, the simple average of the win-rates from the two perspectives is applied. For the purposes of this work, we additionally filtered the data to include only those archetypes which battled *all other* archetypes present in the meta at least twenty times per reporting period.

B. Deck archetype timelines

Figure 2 gives the timeline — beginning from the end of 2016 through to February 2018 — of the *Druid*-based decks present in the meta, with each particular archetype (14 in total) given on the left hand side as they appear in chronological order. The horizontal axis corresponds to the *Data Reaper Report* that the data is drawn from. Each black horizontal bar designates the appearance of that particular archetype in the meta over the appropriate time period. Each vertical line represents a specific change to the system which shall be applied throughout this document: **unbroken lines** indicate the release of an expansion (with new cards and potentially game mechanics) *in addition to* a rotation of a significant proportion of older cards out of the standard mode; **dot-dashed lines** signify the release of an expansion; and, **dotted lines** signify release of balance patches (changes to a number of existing cards). Suffice to say, there is a narrative behind the

time-dependent appearances, and disappearances of each of the listed archetypes in Figure 2.

As a specific example, we focus on the change that occurred between reports 43 and 44 with the release of the *Journey to Un'Goro* expansion — which introduced 135 new cards (some with new play mechanics) to the game. Additionally, a card rotation occurred during this time, making a sizable proportion of cards released prior to 2016 unusable in the standard play format — 208 in all. Such rotations — which happen yearly around April — are designed to keep the game fresh, preventing certain powerful cards and tactics from dominating the meta for too long, and allowing new content to be released without requiring to account for all previously released cards when testing for overpowered tactics.

Two of the rotated cards, *Emperor Thaurissan* and *Aviana*, were cards that greatly improved the viability of *Malygos Druid*; hence the extinction of this archetype past $T = 44$ in Figure 2 could be anticipated. On the other hand, player experimentation also occurred due to the release of new content, with two additional archetypes seeing significant play — *Ramp Druid* and *Token Druid*. While *Ramp Druid* lost popularity with players soon-after, *Token Druid* continued as a popular *Druid* deck until a patch released between reports 55 and 56 *nerfed* the card *The Crystal Core*. This patch greatly affected the archetype *Crystal Rogue*, causing it to fall out of the meta. *Crystal Rogue* was one of *Jade Druid*'s worst match-ups, in addition to being a very favourable one for *Token Druid*. This flow-on effect led to the eventual disappearance of the *Token Druid*, and further cemented the *Jade Druid*'s popularity in the meta.

The history of *Hearthstone*'s meta is full of such narratives, where both small and large system-wide changes lead to extensive disruption in the meta. As previously mentioned, such disruptive elements include the extinction of previously popular decks, the emergence of new decks and the re-emergence of previously extinct decks. Obtaining complete understanding of these changes over time is a non-trivial process, requiring both a large amount of highly dynamic data (we reiterate that Figure 2 is only a small proportion of the entire picture, presenting only one of nine character classes over a limited window of time) and a large degree of subject matter expertise to appreciate the context and changes of the data. Further on in this section we present the (entire) data through the entirely different lens of Shannon entropy. Although such entropy measures somewhat obfuscate the underlying data and eliminate much of the nuance showcased in the narrative surrounding Figure 2, Shannon entropy in particular comes with the benefit of characterising the underlying complexity in the system [40]. This additionally enables non-subject matter experts to appreciate the effects brought about by system-wide changes.

C. Deck frequencies and win-rates

In this section we discuss in more detail the two types of data that are analysed in this work: the frequencies that each of the particular archetypes are played per reporting period T ,

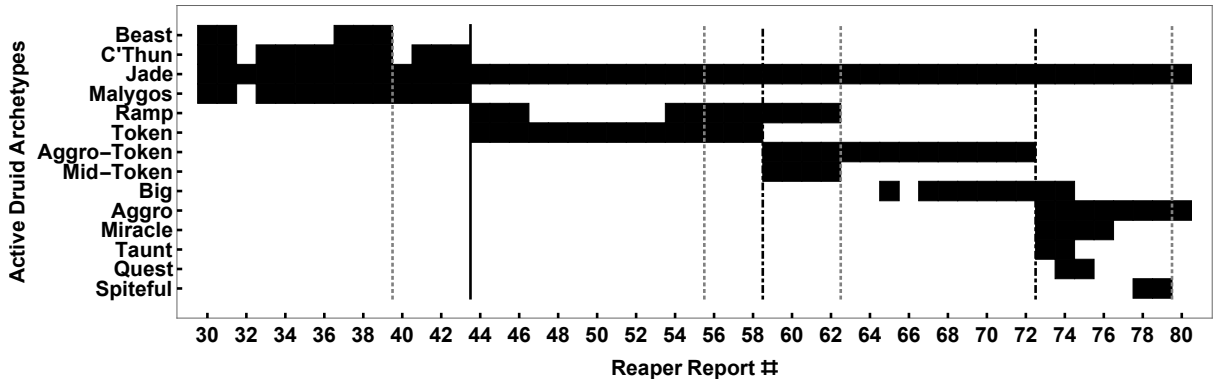


FIG. 2: Timeline of the *Druid*-based deck archetypes present in the meta. Vertical lines represent system changes by the publisher — **unbroken lines** signify release of an expansion (new cards and game mechanics) *in addition to* a rotation of a number of older cards out of the standard mode; **dot-dashed lines** signify the release of an expansion; and, **dotted lines** signify release of balance patches (changes to existing cards). The horizontal axis corresponds to the *Data Reaper Report* from which the data is drawn. The data for the first entry, report 30, was collected over the period 14-20 December 2016. The data for the final entry, report 80, was collected over the period 6-13 February 2018.

and their corresponding win-rates against each other. Beginning with the deck frequencies, we label the set of all active decks in the *Hearthstone* meta for a particular reporting period T as

$$\mathcal{X}^T = \{X_1^T, X_2^T, \dots, X_N^T\}, \quad T \in \{30, 149\}, \quad (5)$$

where each X_i^T denotes a specific active deck archetype currently in the meta for time period T , and we label $N \equiv |\mathcal{X}^T|$. Reiterating, $T \in \{30, 149\}$ corresponds to the *Data Reaper Report* number that the data was drawn from [38], and accounts for approximately three years of *Hearthstone* data, with deck frequency data for $T = 30$ and $T = 149$ being collected over the periods 14–20 December 2016 and 19–27 December 2019, respectively.

For each deck archetype X_i^T , we label the frequency that it was played in time period T as $\mathcal{P}(X_i^T)$. For all $X_i^T \in \mathcal{X}^T$ the complete set of \mathcal{P} forms a discrete probability distribution with the property

$$\sum_{i=1}^{|\mathcal{X}^T|} \mathcal{P}(X_i^T) = 1. \quad (6)$$

In Figure 3 we give the frequencies of the active deck archetypes played over the period 10–18 April 2017, representing $T = 44$ in Eq.(5). In this figure we can see all character classes represented in the 26 active deck archetypes, with the most frequently played archetype — *Midrange Hunter* — being the only *Hunter* character class deck in the meta for that period.

In addition to the frequency that each deck archetype is played, in this work we also consider their win-rates when the decks are played against each other. We label this data $\mathcal{P}(W|P_{X_i^T}, A_{X_j^T})$, which denotes the conditional probability of *winning*, given that the *player* (P) chooses deck X_i and faces an *adversary* (A) using deck X_j , at time period T . As explained in Section II A regarding win-rates data collection

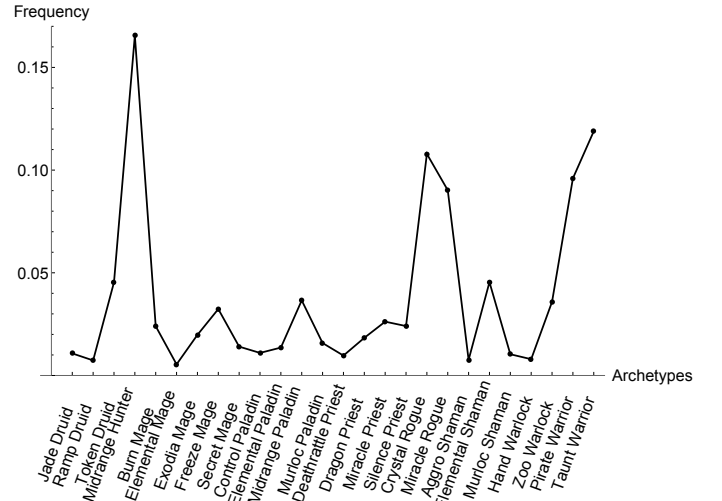


FIG. 3: Deck archetype frequency data for $T = 44$, collected over 10–18 April 2017.

and preparation, win-rates and their transpose are necessarily equal to unity, leading to the identity

$$\begin{aligned} \mathcal{P}(W|P_{X_i^T}, A_{X_j^T}) &= 1 - \mathcal{P}(W|P_{X_j^T}, A_{X_i^T}), \\ \Rightarrow \mathcal{P}(W|P_{X_j^T}, A_{X_i^T}) &= \mathcal{P}(L|P_{X_i^T}, A_{X_j^T}), \end{aligned} \quad (7)$$

for $W = \textit{win}$ and $L = \textit{lose}$. Additionally each match-up with the same archetype is equal to 0.5, *i.e.*

$$\mathcal{P}(W|P_{X_i^T}, A_{X_i^T}) = \mathcal{P}(L|P_{X_i^T}, A_{X_i^T}) = 0.5, \quad (8)$$

meaning that the outcome of *mirror match-ups* are effectively random.

D. Shannon information entropy

In this section we analyse the deck frequencies through the lens of Shannon information entropy, measured via

$$\mathcal{H}(\mathcal{X}^T) = - \sum_{i=1}^{|\mathcal{X}^T|} \mathcal{P}(X_i^T) \log_2 \mathcal{P}(X_i^T). \quad (9)$$

Generally, exactly uniformly distributed probabilities (*i.e.* $\mathcal{P}(X_i) = 1/|\mathcal{X}| \forall X_i \in \mathcal{X}$) will result in maximum entropy values of $\log_2 |\mathcal{X}|$. Thus we can intuitively understand Eq.(9) as an approximate guide to how evenly distributed the archetypes in the meta are over any given reporting period if we compare the actual value to its theoretical maximum

$$\mathcal{H}_{max}(\mathcal{X}^T) = \log_2 |\mathcal{X}^T| \quad (10)$$

which is simply the logarithm of the number of active deck archetypes in the meta for any given time period T .

In Figure 4 we present the Shannon information entropy (unbroken line) and the corresponding maximum entropy (broken line) derived from the frequencies that deck archetypes are played over each of the reporting periods. As explained in Section II B, vertical lines represent specific changes to the system — **unbroken lines** signify expansion releases *in addition to* card rotations; **dot-dashed lines** indicate expansion releases; and **dotted lines** indicate balance patch releases.

A noticeable feature of this figure is that the actual entropy \mathcal{H} and the theoretical maximum \mathcal{H}_{max} largely mirror each other over the entire time period, both in their general trends and when the system experiences sharp variations in both entropy values. Indeed, for both entropy values in the figure, one general trend which persists across the entire data set is that most of the variability, both increase and decrease, occurs immediately after a system-wide change has occurred. The most common of these occurrences is a sharp increase, which is then followed by a marked decrease in entropy immediately after, until the next system-wide change occurs. This particular behaviour in entropy indicates a marked escalation in archetype experimentation immediately after changes occur, with system entropy decreasing soon-after due to players understanding and exploiting strong card synergies and tactics which have emerged due to the changes. For the majority of Figure 4, this behaviour in entropy — and the assumed player behaviour it stems from — is replicated semi-consistently.

Highlighting the instances where change led to a marked decrease in entropy values, we focus on the changes that occurred between both $T = 55$ and 56 , and $T = 62$ and 63 . As previously mentioned in Section II B, between $T = 55$ and 56 in July 2017 a balance patch nerfed the card *The Crystal Core*, which led to the extinction of the relatively powerful *Crystal Rogue* archetype from the meta. In addition to this however, a number of other archetypes were absent from the meta immediately after this change, with only the new *Jade Rogue* archetype emerging, significantly decreasing the amount of active decks. A similar situation happened between $T = 62$ and 63 in September 2017 when a balance patch

nerfed five cards, whose greatest impact negatively affected the frequency that *Druid*-based decks were chosen by players. Specifically, the *Mid-Token Druid* and *Ramp Druid* (amongst others) were extinguished from the meta altogether, with only the new *Tempo Rogue* archetype emerging during this period. This leads us to the observation that, unlike the large scale changes which appear to *generally* increase entropy, events which corresponded to decreases in system entropy are *generally* relatively small changes which largely targeted a small number of archetypes perceived to be overpowered. We do however see marked decreases in entropy values for the major changes caused by the release of the *Rastakhan's Rumble* (between $T = 113$ and 114 in December 2018) and *Rise of the Shadows* (between $T = 125$ and 126 in April 2019) expansions. Even though these expansions both introduced 135 new cards, unlike other expansions their effect led to a reduction of the system's entropy as they both saw a drop in active archetypes present in the meta. This entropy decrease was more significant for *Rise of Shadows* in April 2019 as the expansion was coupled with a card rotation which saw a sizable proportion of cards released two years prior becoming unplayable in the standard game.

In Figure 5 we present the normalised Shannon information entropy $\mathcal{H}(\mathcal{X}^T) = \mathcal{H}(\mathcal{X}^T) / \mathcal{H}_{max}(\mathcal{X}^T)$, derived from deck archetype frequencies played over the reporting periods, with vertical representing system changes as explained in Figure 4. As with the entropy values displayed in Figure 4, an interesting feature for this graph are the sharp variations when changes are enacted on the system. We conjecture that the evolution of the normalised Shannon entropy over time in Figure 5 — cycling through periods of relatively low and high values and spending the majority of its time at intermediate values — shows hallmark signs of a system at criticality [13, 14] — that is, the system appears able to respond and adapt to a rapidly changing environment. Relatively high values indicate that all active deck archetypes are equally popular. If we assume that player choice is naturally heavily based on obtaining victory — and deck popularity is synonymous with its viability — in this case player choice would offer little significance as all active archetypes would have equal probability of being victorious, with players facing a wide variety of equally viable tactics. Conversely, relatively low values indicate that only a small number of active archetypes are able to regularly obtain victory, and player choice would be heavily biased towards those few decks with experimentation kept to a minimum. We argue that system-wide changes are initiated to actively keep it away from these extreme situations: too much choice denying players any agency, or too little choice making the game feel stale — it has been highlighted that *Hearthstone* publishers *Blizzard* specifically releases patches to avoid this scenario [6]. The final case where normalised Shannon entropy values are not relatively high *or* low, and where the trajectory in Figure 5 spends the majority of its time, indicates a scenario where there are a range of viable deck options, but player choice is not arbitrary as not all decks perform as well as each other. This scenario is reminiscent of Crutchfield and Young's [24] concept of the *complexity spectrum* where a system displays the most complexity between its minimum and

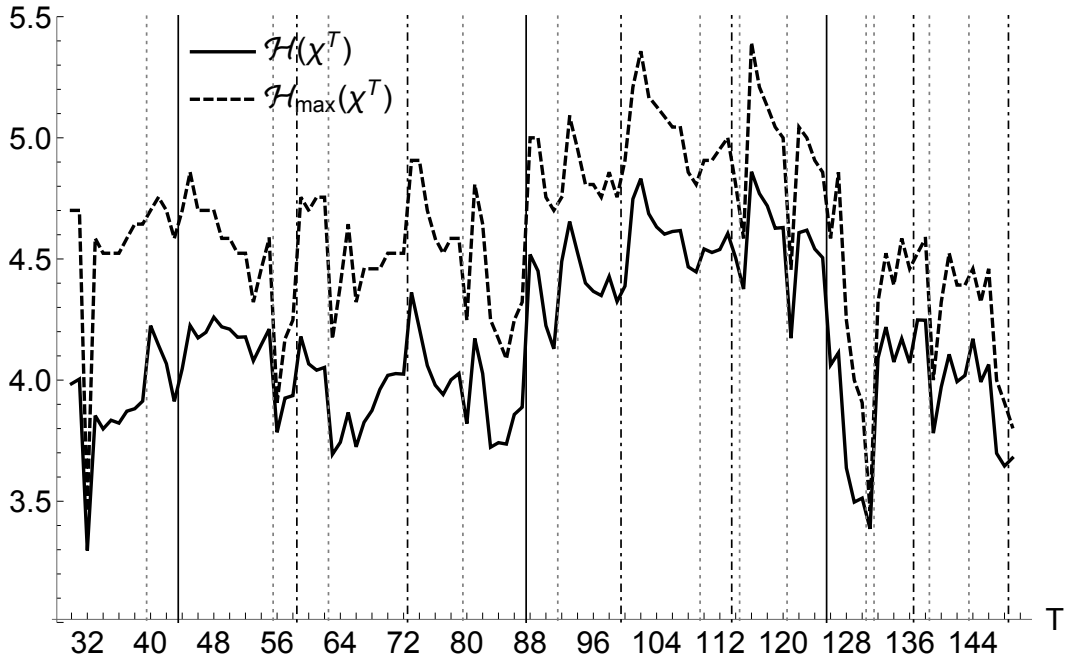


FIG. 4: Graph of the Shannon information entropy (unbroken line) and its theoretical maximum (dashed line) — defined in Eq.(9) and (10) respectively — derived from the frequencies that deck archetypes are played over each of the reporting periods. As articulated in Figure 2, vertical lines represent system-wide changes occurring between reporting periods — **unbroken lines** signify expansion releases *in addition to* card rotations; **dot-dashed lines** indicate expansion releases and **dotted lines** indicate balance patch releases.

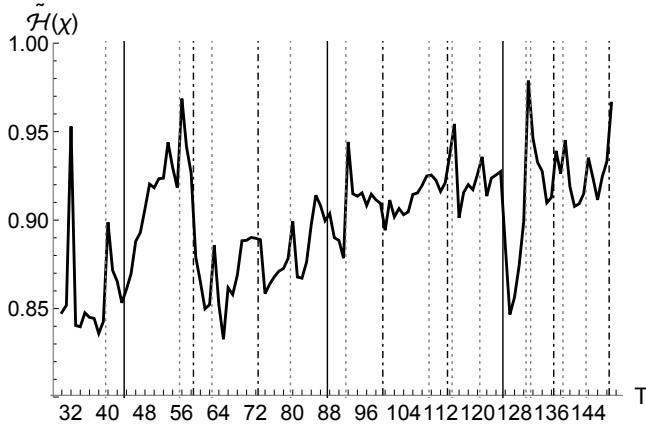


FIG. 5: Graph of the normalised Shannon information entropy — $\tilde{\mathcal{H}}$ — of the frequencies that deck archetypes are played over the various reporting periods. As with Figure 4, vertical lines represent system changes occurring between reporting periods.

maximum normalised Shannon entropy values.

III. INFORMATION STORAGE AND UNDERSTANDING PLAYER CHOICE

A. Local active information storage applied to archetype choices

Focusing on the LAIS definition given in Eq.(1), in the absence of tracking game-by-game deck choices made by players across a substantial period of time, it will be necessary to estimate the conditional probability that a certain deck is chosen in a specific reporting period, given the previous distribution of chosen decks, and their win-rates in the past reporting period(s). Importantly, the artificial conditional probabilities will be constructed following assumptions which can be interpreted to simulate understandable player behaviour. Once we have the constructed conditional probabilities, we can then apply Eq.(1) to test how well our assumptions about the method that players make deck archetype choices reflects the data .

Reiterating, the quantity X_i^T denotes the deck archetype X_i from time period T . Naturally, the frequency (or marginal probability) that the deck is chosen in that time period is given by $\mathcal{P}(X_i^T)$. We then construct the set of artificial conditional probabilities $\mathcal{P}(X_i^T | X_{j_1}^{T-1}, \dots, X_{j_K}^{T-K})$ of deck archetype X_i^T being chosen, given that decks $\{X_{j_1}^{T-1}, \dots, X_{j_K}^{T-K}\}$, were played in the past. Importantly, the conditional probabilities

must satisfy the following consistency condition

$$\mathcal{P}(X_i^T) = \left[\prod_{n=1}^K \sum_{j_n=1}^{|\mathcal{X}^{T-n}|} \mathcal{P}(X_{j_n}^{T-n}) \right] \mathcal{P}(X_i^T | X_{j_1}^{T-1}, \dots, X_{j_K}^{T-K}) \quad (11)$$

following Bayes' theorem [12]. Using this notation, the LAIS associated with deck X_i^T , given past choices, is given via

$$a_K(X_i^T | X_{j_1}^{T-1}, \dots, X_{j_K}^{T-K}) = \log_2 \frac{\mathcal{P}(X_i^T | X_{j_1}^{T-1}, \dots, X_{j_K}^{T-K})}{\mathcal{P}(X_i^T)}. \quad (12)$$

In this work we apply the convention that LAIS values are equal to zero if $\mathcal{P}(X_i^T) = 0$ — *i.e.* the deck X_i^T does not appear in the meta for time period T . Additionally the AIS associated with each deck archetype, $A_K^{(deck)}(X_i^T)$, is given as the LAIS expectation value over all past deck choices

$$A_K^{(deck)}(X_i^T) = \left[\prod_{n=1}^K \sum_{j_n=1}^{|\mathcal{X}^{T-n}|} \mathcal{P}(X_{j_n}^{T-n}) \right] \times \mathcal{P}(X_i^T | X_{j_1}^{T-1}, \dots, X_{j_K}^{T-K}) a_K(X_i^T | X_{j_1}^{T-1}, \dots, X_{j_K}^{T-K}). \quad (13)$$

We remark that deck-AIS values in Eq.(13) are equivalent to the definition of *agent rigidity* given in [36]. Also necessary is the total AIS for each time period, A_K^T , which is the LAIS expectation value over all past and current deck choices

$$A_K^T = \sum_{i=1}^{|\mathcal{X}^T|} A_K^{(deck)}(X_i^T). \quad (14)$$

Thus using the concepts of AIS and its relation to Shannon entropy outlined in Eq.(4), we construct a number of instances of conditional probabilities based on assumptions which can be interpreted as relatively simple simulations of player behaviour. In this work we test whether the past *Hearthstone* deck-frequency and win-rate data can be used to account for the complexity witnessed in the system by testing whether the generated AIS values compare favourably with the Shannon entropy of Section IID. By extension, this tests whether the CCG players base their deck choices on past game data.

B. Weightings applied to construct conditional probabilities

To generate the set of conditional probabilities we are initially guided by the assumption that player decision-making is solely influenced by comparing the past deck-frequency or win-rate data and adjust their decks accordingly. In section III D we shall combine these assumptions into a single weighting.

Thus, if a player chooses deck X_j in time period $T-1$, then the probability that the player chooses X_i in the next time period T is weighted by a function of both decks in the previous time period. This is expressed mathematically via

$$\mathcal{P}(X_i^T | X_j^{T-1}) = \varepsilon^{(i)} \mathcal{P}(X_i^T) \mathcal{H}_{T-1}(i|j), \quad (15)$$

where $\mathcal{H}_{T-1}(i|j) = f(X_i^{T-1}, X_j^{T-1})$.

The weighting \mathcal{H} compares either deck-frequencies, and/or the win-rates that players experienced against deck X_i given they played deck X_j in time period $T-1$. The function f generally offers a larger weight if the deck X_i was played more frequently, or had a higher win-rate against X_j . Additionally, the coefficient $\varepsilon^{(i)}$ is to ensure that the consistency condition given by Eq.(11) is satisfied. In order to test the assumption over multiple K -time periods it is elementary to generalise the construction of the conditional probabilities via

$$\mathcal{P}(X_i^T | X_{j_1}^{T-1}, \dots, X_{j_K}^{T-K}) = \varepsilon^{(i)} \mathcal{P}(X_i^T) \prod_{n=1}^K \mathcal{H}_{T-n}(i|j_n), \quad (16)$$

with the weighting factors \mathcal{H} defined in Eq.(15). The conditional probability given in Eq.(16) factors into how the deck archetype X_i^{T-n} compared with the decks $X_{j_n}^{T-n}$ over all K time periods and modifies the marginal probability of choosing deck archetype X_i^T accordingly. Additionally, by ensuring that the consistency condition given in Eq.(11) is adhered to, the coefficients $\varepsilon^{(i)}$ are given as the following

$$\varepsilon^{(i)} = \prod_{n=1}^K \left\{ \sum_{j_n=1}^{|\mathcal{X}^{T-n}|} \mathcal{P}(X_{j_n}^{T-n}) \mathcal{H}_{T-n}(i|j_n) \right\}^{-1}, \quad (17)$$

Thus, over a general number of K time periods, the AIS associated with each deck, X_i^T , for this assumption is given via

$$A_K^{(deck)}(X_i^T) = \left[\prod_{n=1}^K \sum_{j_n=1}^{|\mathcal{X}^{T-n}|} \mathcal{P}(X_{j_n}^{T-n}) \mathcal{H}_{T-n}(i|j_n) \right] \times \varepsilon^{(i)} \mathcal{P}(X_i^T) \log_2 \varepsilon^{(i)} \prod_{n=1}^K \mathcal{H}_{T-n}(i|j_n). \quad (18)$$

with the AIS for the entire time period T given by Eq.(14).

In Eq.(19) we give the exact forms of the weighting functions applied in Eq.(16) when considering past deck-frequencies f_{FR} :

$$f_{FR}(\Delta\mathcal{P}) = Char_{i,j} \times \begin{cases} e^{2\text{sgn}(\Delta\mathcal{P})|\Delta\mathcal{P}|} \\ e^{\text{sgn}(\Delta\mathcal{P})|\frac{\Delta\mathcal{P}}{0.2}|^2} \\ e^{2\text{sgn}(\Delta\mathcal{P})|\Delta\mathcal{P}|^{\frac{1}{2}}} \\ e^{2\text{sgn}(\Delta\mathcal{P})|\Delta\mathcal{P}|^{\frac{1}{4}}} \end{cases} \quad (19)$$

$$\text{where } \Delta\mathcal{P} = \begin{cases} \mathcal{P}(X_i^{T-1}) - \mathcal{P}(X_j^{T-1}) & i \neq j, \\ \mathcal{P}(X_i^{T-1}) - \bar{\mathcal{P}}(\mathcal{X}^{T-1}) & i = j. \end{cases}$$

and

$$\bar{\mathcal{P}}(\mathcal{X}^{T-1}) = \sum_{k=1}^{|\mathcal{X}^{T-1}|} \frac{\mathcal{P}(X_k^{T-1})}{|\mathcal{X}^{T-1}|} \quad (20)$$

is the mean value of the deck-frequencies played over time-period $T-1$. Importantly, the term $Char_{i,j}$ in Eq.(19) is a multiplicative factor which checks the *character class* of both

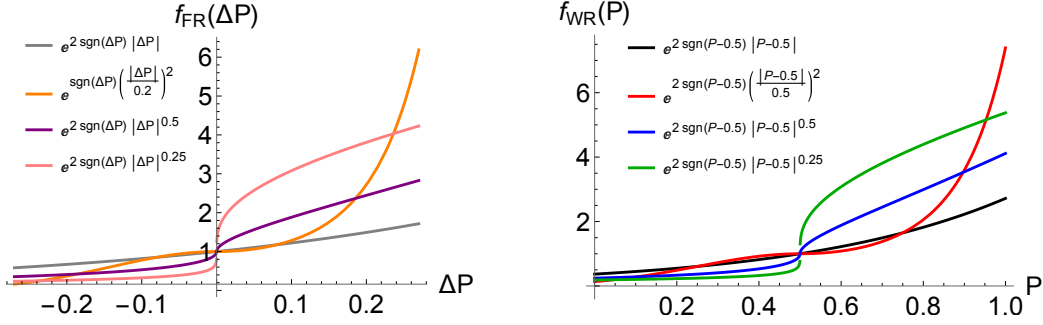


FIG. 6: Plots of the specific forms of the functional responses applied to the weightings in Eq.(15). Left panel shows deck-frequencies f_{FR} detailed in Eq.(19), and the right panel shows win-rates f_{WR} detailed in Eq.(21).

decks X_i^{T-1} and X_j^{T-1} , and returns a value greater than unity if the character classes are equal, or 1 if not. As explained in Section ID each of the character classes gain access to class specific cards which require a resource investment to both obtain, and learn how play effectively. Thus the term $Char_{i,j}$ simulates the *resource hurdle* and/or *unwillingness* involved in changing character classes. For this work we set $Char_{i,i} = 2$ — meaning that we assume players are doubly likely to choose a deck if it is the same character class as the deck they played in the previous time period.

Correspondingly, in Eq.(21) we give the exact forms of the weighting functions applied in Eq.(16) when considering past win-rates f_{WR} :

$$f_{WR}(\mathcal{P}) = \begin{cases} e^{2\text{sgn}(\mathcal{P}-0.5)|\mathcal{P}-0.5|} \\ e^{2\text{sgn}(\mathcal{P}-0.5)\left(\frac{\mathcal{P}-0.5}{0.5}\right)^2} \\ e^{2\text{sgn}(\mathcal{P}-0.5)|\mathcal{P}-0.5|^{\frac{1}{2}}} \\ e^{2\text{sgn}(\mathcal{P}-0.5)|\mathcal{P}-0.5|^{\frac{1}{4}}} \end{cases} \quad (21)$$

where $\mathcal{P} = \begin{cases} \mathcal{P}(L|P_{X_j^{T-1}}, A_{X_i^{T-1}}) & i \neq j, \\ \bar{\mathcal{P}}(L|P_{\mathcal{P}^{T-1}}, A_{X_i^{T-1}}) & i = j, \end{cases}$

and

$$\bar{\mathcal{P}}(L|P_{\mathcal{P}^{T-1}}, A_{X_i^{T-1}}) = \sum_{k=1}^{|\mathcal{P}^{T-1}|} \mathcal{P}(X_k^{T-1}) \mathcal{P}(L|P_{X_k^{T-1}}, A_{X_i^{T-1}}) \quad (22)$$

is the mean value of the win-rate for deck X_i over time-period $T-1$.

In Figure 6 we graph the functional responses applied to the weightings in Eq.(19) (left panel) and Eq.(21) (right panel). Specifically, the grey and black trajectories in the left and right panels respectively, display an almost-linear response, meaning that the probability of choosing deck X_i effectively rises linearly the more it was played (left panel) and the better it performed against (right panel) deck X_j in the previous time period. The remaining coloured trajectories correspond to decidedly more non-linear responses. In the left hand plot

measuring deck-frequency differences, if the difference is less than 0 then the exponential has a negative argument and the weighting is minimal. If the frequency difference is greater than 0 however, the argument is positive and the weighting grows non-linearly as a function of the difference; the quadratic weighting in orange grows more slowly initially, but then experiences the sharpest rise as $\Delta\mathcal{P} \rightarrow 0.27$; we choose this range as the largest frequency — occurring at $T = 129$ — being *Lackey Rogue* being chosen 26.5% of the time. Contrast to this, the pink trajectory experiences its sharpest rise immediately after $\Delta\mathcal{P} = 0$, with a steady — almost linear — rise after this point, with the purple trajectory offering a somewhat subdued version of the pink trajectory. We see an equivalent picture with the four trajectories on the right hand panel of Figure 6. Measuring the win-rate between decks, if the win-rate is less than 50% then the exponentials have a negative argument, leading to minimal weighting. If the win-rate is greater than 50% the arguments are positive and the weightings grow non-linearly, for all but the black trajectories. Mirroring the left hand panel, the quadratic weighting in red grows more slowly initially, but then experiences the sharpest rise as $\mathcal{P} \rightarrow 1$; we choose this range as the largest win-rate — occurring at $T = 123$ — being *Taunt Warrior* winning against *Cube Rogue* 96.7% of the time.

C. Comparing deck frequencies and win-rates individually

In Figure 7 we plot the total AIS defined in Eq.(14) under the assumption that deck choices for T are based on results from $T-1$ — *i.e.* $K = 1$ in Eq.(14). Furthermore, the functional responses of the past frequencies are the same as those given in Eq.(19), with the colours of each trajectory matching the colours given to each functional response in the left panel of Figure 6.

A major feature of Figure 7 is the marked difference between the AIS values with different functional responses. Specifically, we see that the almost-linear (grey) and squared (orange) responses display similar AIS values — except at $T \in (124, 132)$, where the orange and purple responses obtain similar values. Nevertheless, the highest AIS values are

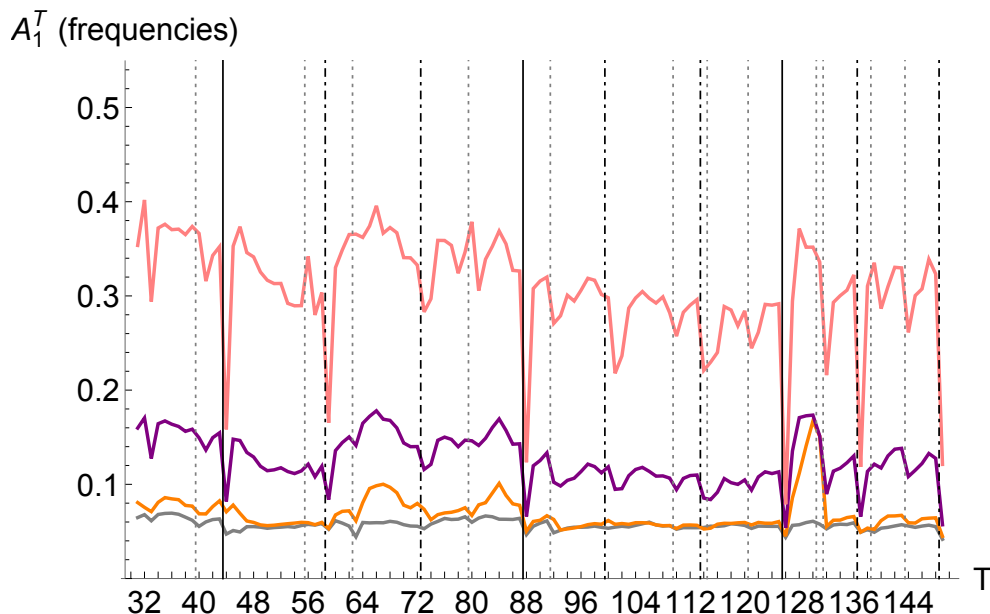


FIG. 7: Plots of Eq.(14) which gives total AIS associated with each time period. Each trajectory was calculated assuming deck choices are based on deck-frequencies of $T - 1$ — *i.e.* $K = 1$ in Eq.(14) — and the functional responses of the past deck frequencies given in Eq.(19). Note that the colours for each trajectory corresponds with the colours given to each deck-frequency functional response on the left panel of Figure 6.

obtained by the pink trajectory, whose functional response rises the sharpest as the difference between the frequencies becomes greater than 0 and positive, as witnessed in the left panel of Figure 6. Thus, out of the four functional responses based on deck-frequency that we have considered, the one which best aligns with actual player behaviour is the one which rises the sharpest immediately after the deck under consideration compares favourably. This suggests that the size of the frequency difference matters less than the simple fact that one deck frequency X_i^{T-1} compares favourably to X_j^{T-1} , with $\Delta\mathcal{P} > 0$.

An additional feature of Figure 7 is that the AIS values experience a significant decrease whenever they cross time periods where major change is introduced into the system — indicated by the unbroken and dot-dashed vertical lines. One interpretation of this phenomenon is that when such change is introduced into the system, players base significantly less of their decision-making on past results — at least compared to their previous deck choices. We illustrate this phenomenon, and the underlying causes, by detailing the five changes which happened between $T = 39$ and $T = 63$. Beginning with the change between $T = 39$ and $T = 40$, at the end of February 2017 a patch was released which nerfed the cards *Small Time Buccaneer* and *Spirit Claws*. Arguably, this was a targeted change whose main consequence was to break the dominance of the seemingly overpowered *Aggro Shaman* archetype in the meta. This patch, as well as the patches released between $T = 55$ and $T = 56$ (July 2017), and $T = 62$ and $T = 63$ (September 2017) — whose consequences were discussed in Sections II B and II D — only affected a handful of cards and were largely targeting a small number of archetypes. Though such small changes

have the potential to substantially change the meta and its corresponding Shannon entropy, as shown in Figures 3 and 4, these changes do not seem to substantially change the underlying decision-making players employ to choose decks, as they have very little effect on the AIS values for all the functional responses. Indeed, we can see that AIS values actually increased between $T = 55$ and $T = 56$, effectively meaning this change actually *reinforced* past decision-making.

Nevertheless, we see a starkly different picture in Figure 7 between $T = 43$ and $T = 44$ (April 2017) and between $T = 58$ and $T = 59$ (August 2017), with the release of the *Journey to Un'goro* and *Knights of the Frozen Throne* expansions, respectively. Both of these expansions introduced extensive changes, including new game mechanics and 135 new cards per expansion. In both of these instances we witness marked drops in AIS values, meaning that the assumption that players base their deck choices on past results is especially incorrect when changes of such magnitude are introduced. In fact, all of the major decreases in AIS values occur immediately after significant changes are introduced, from the *Kobolds and Catacombs* expansion just before $T = 73$ (December 2017), to the *Descent of Dragons* expansion just before $T = 149$ (December 2019) — both of which introduce over 130 new cards into play.

In Figure 8 we again plot the total AIS defined in Eq.(14), under the assumption that player deck choices for T are based on past win-rates from $T - 1$. The functional responses of the past win-rates are given in Eq.(21), with the colours of each trajectory in Figure 8 matching the colours given to each functional response in the right panel of Figure 6. Aside from the AIS values being overall slightly higher — suggesting that

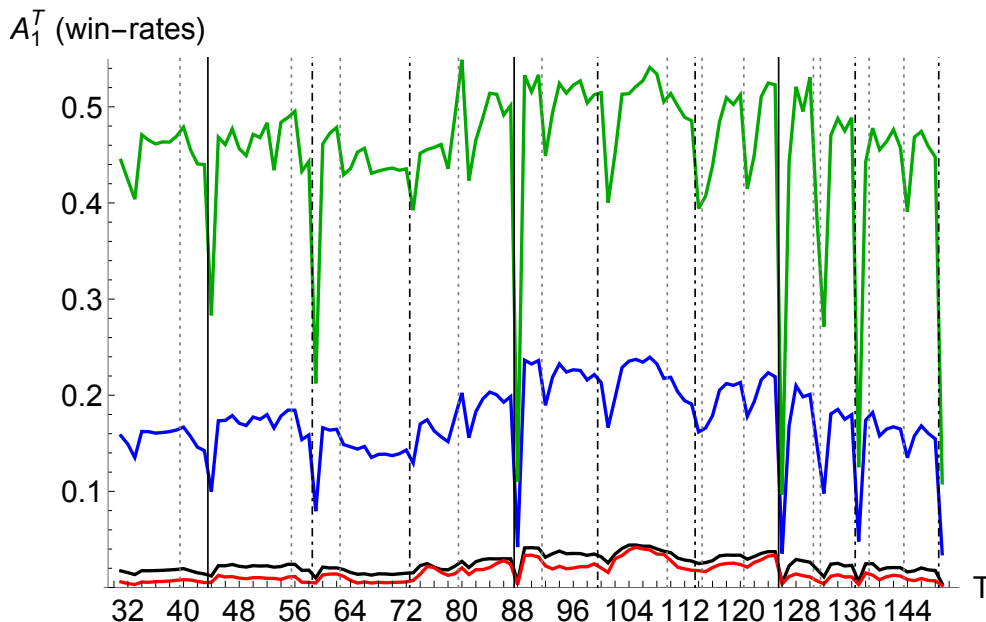


FIG. 8: Plots of the total AIS associated with each time period. Each trajectory was calculated assuming deck choices are based on win-rates of $T - 1$ and the functional responses of the past win-rates given in Eq.(21). Note that the colours for each trajectory corresponds to the colours given to each win-rate functional response on the right panel of Figure 6.

past win-rates are perhaps a more appropriate measure than past deck frequencies in determining player decision-making — we note that Figure 8 displays much of the same features already discussed in Figure 7. Again, we see that the almost-linear (black) and squared (red) responses display similar AIS values, with the highest AIS values obtained by the green trajectory, whose functional response rises the most as the win-rate between the decks being compared becomes greater than 50%, as seen in the right panel of Figure 6. Again, the functional response which best aligns with actual player behaviour is the one which rises the sharpest immediately after the win-rate of the deck under consideration performs favourably with the deck it is being compared to. Furthermore, similar to Figure 7 we see that the AIS values in Figure 8 experience notable decreases whenever they cross time periods where significant change is introduced into the system, and subdued responses (or even increases) when crossing time periods where minor change is introduced.

D. Combining deck frequencies and win-rates

By applying the functional responses given in Eqs.(19) and (21), we see that Figures 7 and 8 reveal that past deck-frequencies and win-rates are approximately equally as important as each other in determining player decision-making. In Figure 9 we present the resulting AIS values after combining the two types of functional responses — deck frequencies via Eq.(19) and win-rates via Eq.(21) — into a single func-

tional response given by

$$\mathcal{X}_{T-1}(i|j) = \underbrace{f_{FR}(\Delta\mathcal{P})}_{\text{Eq.(19)}} \times \underbrace{f_{WR}(\mathcal{P})}_{\text{Eq.(21)}}. \quad (23)$$

Each trajectory in Figure 9 is composed of two colours — signifying which of the functional responses were combined on the left hand panel (deck frequencies) and right hand panel (win-rates) of Figure 6. Thus, black-grey denotes the almost-linear responses; red-orange the squared responses; green-pink the responses which rise the sharpest if the difference of deck frequencies is greater than zero and the win-rate is greater than 50%; and finally blue-purple giving the subdued version of the green-pink response.

Macroscopically, the AIS trajectories in Figure 9 are very similar to those previously presented in this work, including noticeable decreases in values immediately after large-scale changes have been initiated. Nevertheless, the main difference brought about by considering both deck frequencies and win-rates in Figure 9 is the marked increase in AIS values. Specifically, we see that the values of the pink and green AIS trajectories in Figures 7 and 8 respectively, have been approximately doubled by their corresponding pink-green AIS trajectory in Figure 9. Indeed, recalling the duality relation between Shannon entropy, AIS and the entropy rate in Eq.(4), if we compare the AIS values in Figure 9 with the Shannon entropy in Figure 4, it is possible to appreciate that approximately 20% of the uncertainty within the *Hearthstone* meta (*i.e.* its Shannon entropy) is explained simply by considering past deck frequencies and win-rates via the functional response given in Eq.(23).

In Figure 10 we plot the exact value of this explainability per time period, given by $A_1^T / \mathcal{H}(\mathcal{X}^T)$, where we have used

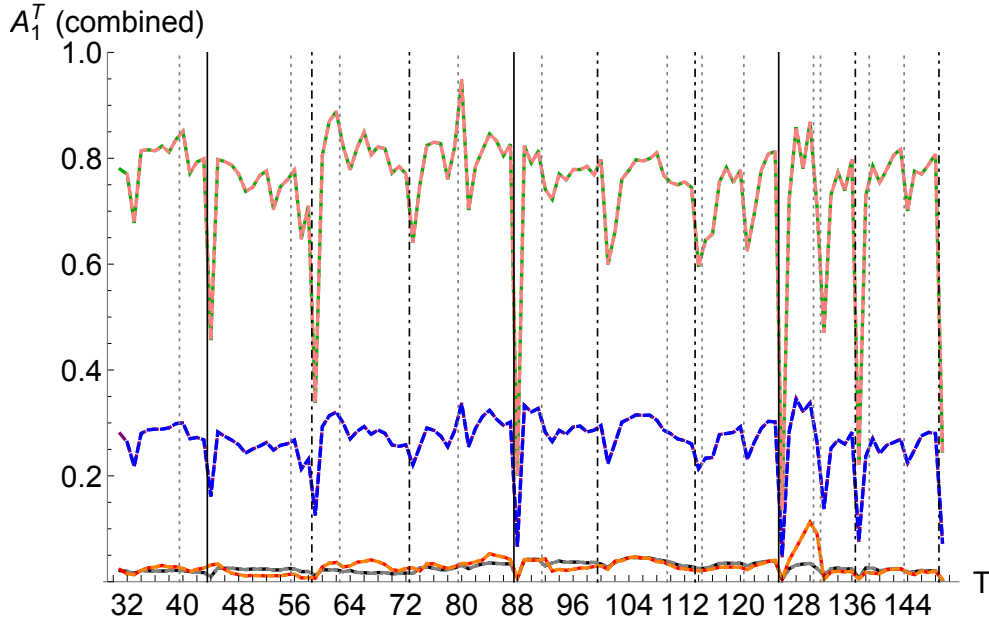


FIG. 9: Plots of Eq.(14) which gives total AIS associated with each time period. Each trajectory was calculated assuming deck choices are based on data from the previous reporting period. The functional responses, given in Eq.(23), compare both deck frequencies and win-rates. We note that each trajectory is now given by two colours — signifying which of the functional responses were combined on the left hand panel (deck frequencies) and right hand panel (win-rates) of Figure 6.

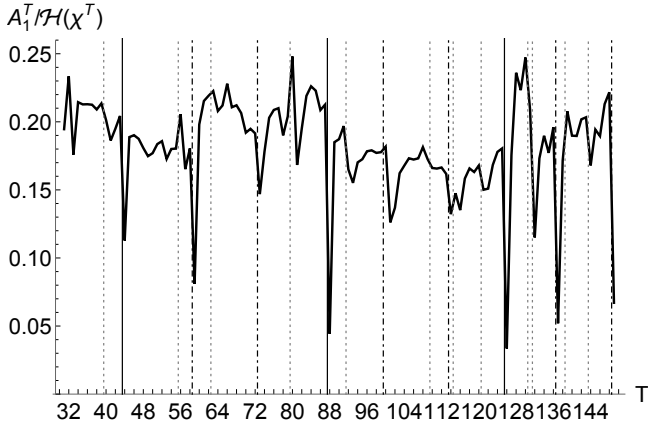


FIG. 10: Plot of the percentage of uncertainty (or surprise) within the *Hearthstone* meta that is explained by considering past deck frequencies and win-rates via the functional response given in Eq.(23).

the highest AIS values for A_1^T , taken from the green-pink trajectory in Figure 9. Reiterating, the value of $A_1^T / \mathcal{H}(X^T)$ varies between $[0, 1]$ for any system; a value close to zero signifying that the assumption(s) used to construct the AIS reveal very little about the uncertainty in the system. Likewise, a value close to unity signifies that the assumption(s) used to construct the AIS offers a near-to-complete explanation of the uncertainty in the system. Our assumptions in Eq.(23) are designed to simulate very simple and understandable player behaviour; basically that players are more likely to choose decks

which have performed better, and played more frequently, in the past. As displayed in Figure 10, for most time periods this simple principle appears to explain approximately 20% of the *Hearthstone* meta data. Though we acknowledge that our assumptions do not take into account the nuances in the choices that players undoubtedly make when faced with deck construction, the fact that AIS values drop so dramatically immediately after large system-wide changes (meaning that relying on past results to construct new decks is erroneous) validates our assumptions. Specifically, we know from our results and discussion in Sections II B and II D that deck construction and tactics experimentation *generally* increases immediately after such changes, leading to the emerging of new archetypes, and the corresponding Shannon entropy. Hence, during these periods it would be incorrect to assume that relying on past results to inform current decisions would lead to good outcomes — dramatic decreases in AIS values during these periods validates these assertions.

E. Active information storage of deck archetypes

In Figure 11 we provide a heat-plot of the deck-AIS values per time period — $A_1^{(deck)}(X_i^T)$ via Eq.(13) — which were used to generate the largest AIS values (pink-green) in Figure 9 — *i.e.* using the combined functional response of Eq.(23) which considers both past deck frequencies and win-rates. The horizontal axis of Figure 11 indicates each of the 166 deck archetypes considered in this study, which are ordered alphabetically within each of the nine character classes, and the vertical axis indicates the relevant time period for that particular

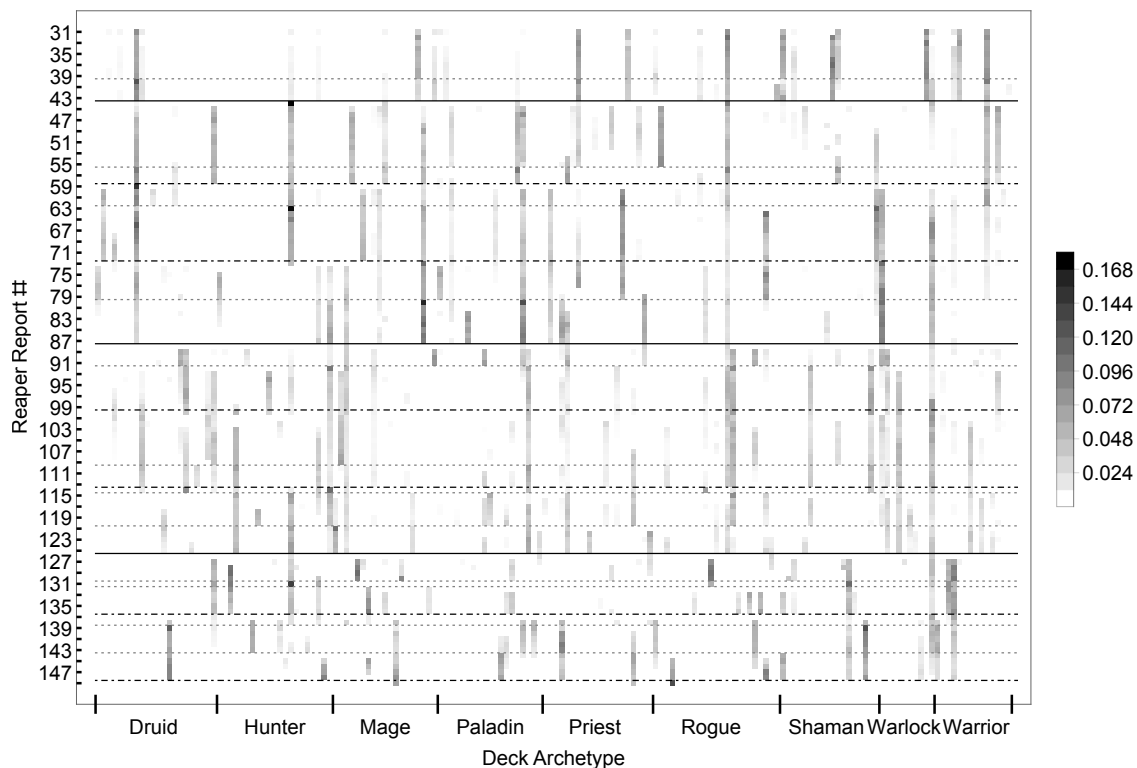


FIG. 11: Plot of Eq.(13), giving the deck-AIS values per time period which were used to generate the pink-green AIS values in Figure 9 — produced using the combined functional response of Eq.(23) which considers both past deck frequencies and win-rates.

archetype’s deck-AIS. Furthermore, horizontal lines in Figure 11 indicate system-wide changes occurring between reporting periods, as per the convention previously detailed in Figures 4–10. White regions signify archetypes that did not contribute deck-AIS values for that particular time period, and dark(er) regions indicate archetypes whose AIS-values are non-zero for the particular time period. Hence these particular decks adhere to the assumption that their frequency of play at time T correlates with their appearance in the meta at time $T - 1$ — the darker the colour, the more pronounced the correlation.

Visual inspection of Figure 11 reveals in greater detail the impact that change has on the various archetypes, as opposed to the macroscopic picture given in Figures 7–10. Explicitly, we see that periods experiencing small system changes generally have minimal effect on both the popularity of the majority of the decks active in the meta, and their specific deck-AIS values. Moreover, time periods experiencing large changes generally display disruptive effects, with a sizeable proportion of archetypes becoming extinct in the meta, and a noticeable change in the deck-AIS values of the archetypes which remain active. Focusing again on the major change occurring between $T = 43$ and 44, in Section III C we noted a sizable drop in total AIS values due to the release of the *Journey to Un’goro* expansion introducing 135 new cards, in addition to 208 previously released cards being made unplayable in standard mode. The impacts of these changes are made clearer in Figure 11, with a number of the active archetypes becom-

ing extinct past $T = 43$. Interestingly, we see that some of the archetypes which do survive the transition to $T = 44$ actually obtain a sizable increase in deck-AIS values, such as the *Midrange Hunter* and to a lesser extent the *Miracle Rogue*. Due to these archetypes surviving the change post expansion release and performing relatively well in the meta, we interpret the relatively large increase in deck-AIS values as these archetypes offering players a means to reinforce their previous decision-making during a disruptive period.

IV. DISCUSSION AND FUTURE WORK

In this work we applied a number of information-theoretic measures to characterise and understand three years of player data — over the 2016–2019 period — of the online CCG *Hearthstone*. Specifically, using the time-dependent frequencies that deck archetypes are played, to generate the system’s Shannon entropy, provided a unique and useful characterisation of the meta. One striking trend which manifested across the majority of the considered time-period was that most of the variability in the entropy appeared immediately after a system-wide change had occurred. For instance, sharp increases in entropy values — usually followed by rapid decreases immediately after — implied a marked escalation in deck experimentation after change had been enacted, with entropy decreasing soon-after due to players understanding and

exploiting the strong decks and tactics which emerged due to changes. Additionally, applying the concept of local active information storage, we constructed artificial conditional probabilities that particular deck archetypes were chosen in the current time-period, based on previous deck distributions and win-rates of the immediate past period. Though the weights used to construct the conditional probabilities were relatively simple, they could be interpreted as a understandable simulation of player decision-making. An undeniable feature emerging from the resulting AIS values were the significant decreases experienced during periods of major change, implying that players base significantly less of their decision-making on past results during disruptive periods. Furthermore, small system changes did not seem to significantly change the underlying decision-making players employed in their archetype choices; in some instances we actually saw an increase in AIS values, implying that such changes effectively reinforced past decision-making.

There are a number of clear avenues to further this work, both for CCGs and wider application areas. With regards to further exploration of CCGs, it may be possible to combine exploration of information transfer entropy and AIS, similar to [36], in an attempt to establish if the *Hearthstone* landscape in Figure 1 displays the primitives (storage and communications) of a universal computer [41], where the millions of *Hearthstone* players act as the system’s corresponding agents/neurons to respond and adapt to the environment. Correspondingly, one could apply *Fisher entropy* [42] in an attempt to uncover control parameter(s) which influences CCG-system criticality. An additional generalisation would include trying to algorithmically-optimize AIS values by producing weights to replace the mathematical functions — Eqs.(19) and (21) — used in this work. This optimisation would undoubtedly come with the challenge of interpreting the results through the lens of player behaviour [43]. It would also be worth considering the impact of constructing conditional

probabilities based on deck choices beyond $T - 1$ — *i.e.* $K > 1$ in Eq.(12). As mentioned in [34] the choice must be made carefully, since using too many past states can result in overestimation of the AIS value. It may also be fruitful to pursue an information-theoretic extension of the algorithmic deck construction work of Fontaine *et al.* [8] by including generalised entropies similar to those considered in Prokopenko *et al.* [44] to maximise synchronisation/coordination in artificial systems with the intent of *information-driven evolutionary design*.

Applying similar methods to other game-related application areas, we posit that it would be possible to gain appreciation of the evolution of other games with online landscapes similar to Figure 1. Indeed, an equivalent analysis of the real-time-strategy-game *Starcraft II*, with its mix of human players and Artificial Intelligence (AI) [45], may offer non-trivial insights on the impacts of AI interacting with wider society. Finally, similar to the work detailed in [46], we hope that the information-theoretic results obtained about the nature of decision-making behaviour in epochs of system-wide change will be used to examine relevant data sets stemming from wider society. Such applications include: understanding the economical impacts of shifts in the international political landscape [47] and awareness of the changing nature of population behaviours [48].

ACKNOWLEDGEMENTS

This work was supported by a Research Fellowship under Defence Science and Technology Group’s Modelling Complex Warfighting strategic research initiative. The authors are grateful to the *Vicious Syndicate* team for agreeing to share their data set for research purposes. We additionally acknowledge Ivan Garanovich, Scott Wheeler, Keeley McKinlay, Carlos Kuhn, Alexander Kalloniatis, Sean Franco and Daniela Schlesier for fruitful discussions, and Mikhail Prokopenko for helpful feedback on an early draft of this work.

-
- [1] Magic: the Gathering. Facts and Figures. <https://magic.wizards.com/en/content/magic-25th-anniversary-page-facts-and-figures>
 - [2] Markowitz H. Portfolio selection. *Journal of Finance*. 1952;7(1):77–91.
 - [3] Harrison K., Elsayed S., Garanovich I., Weir T., Galister M., Boswell S., Taylor R. and Sarke R. Portfolio optimization for defence applications. *IEEE Access*. 2020;8:60152–78.
 - [4] Carter M., Gibbs M. and Harrop M. Metagames, paragames and orthogames: a new vocabulary. In: El-Nasr M., Consalvo M. and Feiner S. editors *International Conference on the Foundations of Digital Games* Raleigh, NC, USA, May 29–June 01. ACM 2012 p. 11–7.
 - [5] García-Sánchez P., Tonda A., Squillero G., Mora A. and Merelo J. Evolutionary deckbuilding in *Hearthstone*. In: *Symposium on Computational Intelligence and Games*. Santorini, Greece, September 20–23. IEEE 2016.
 - [6] Bursztein E. I am a legend: Hacking *Hearthstone* using statistical learning methods. In: *Symposium on Computational Intelligence and Games*. Santorini, Greece, September 20–23. IEEE 2016.
 - [7] Stiegler A., Messerschmidt C., Maucher J. and Keshav D. *Hearthstone* deck-construction with a utility system. In: *10th International Conference on Software, Knowledge, Information Management and Applications*. Chengdu, China, December 15–17. IEEE 2016 p. 21–8.
 - [8] Fontaine M., Lee S., Soros L., de Mesentier Silva F., Togelius J. and Hoover A. Mapping *Hearthstone* deck spaces through MAP-elites with sliding boundaries. In: *Proceedings of the Genetic and Evolutionary Computation Conference*. Prague, Czech Republic, July 13–17. ACM 2019 p. 161–9.
 - [9] Bhatt A., Lee S., de Mesentier Silva F., Watson C., Togelius J. and Hoover A. Exploring the *Hearthstone* deck space. In: *Proceedings of the 13th International Conference on the Foundations of Digital Games* Malmö, Sweden, August 7–10. ACM 2018.
 - [10] de Mesentier Silva F., Canaan R., Lee S., Fontaine M., Togelius J. and Hoover A. Evolving the *Hearthstone* meta. In: *IEEE Con-*

- ference on Games. London, UK, August 20–23. IEEE 2019.
- [11] Wikipedia: Gameplay of Hearthstone. https://en.wikipedia.org/wiki/Gameplay_of_Hearthstone
- [12] MacKay D. *Information Theory, Inference, and Learning Algorithms*. (Cambridge University Press: Cambridge) 2003.
- [13] Hohenberg P. and Halperin B. Theory of dynamic critical phenomena. *Reviews of Modern Physics* 1977;**49**:435–79.
- [14] Roli A., Villani M., Filisetti A. and Serra R. Dynamical criticality: Overview and open questions. *Journal of Systems Science and Complexity*. 2018;**31**:647–63.
- [15] Kalloniatis A., Zuparic M. and Prokopenko M. Fisher information and criticality in the Kuramoto model of nonidentical oscillators. *Physical Review E*. 2018;**98**:022302.
- [16] Baym M. and Hübler A. Conserved quantities and adaptation to the edge of chaos. *Physical Review E*. 2011;**73**:056210.
- [17] Polani D. Foundations and formalizations of self-organization. In: Prokopenko M. editor *Advances in Applied Self-Organizing Systems*. (Springer: London) 2013 p. 23–42.
- [18] Mora T. and Bialek W. Are biological systems poised at criticality? *Journal of Statistical Physics* 2011;**144**:268–302.
- [19] Balleza E., Alvarez-Buylla E., Chaos A., Kauffman S., Shmulevich I. and Aldana M. Critical dynamics in genetic regulatory networks: Examples from four kingdoms. *PLoS ONE*. 2008;**3**(6):1–10.
- [20] Langton C. Computation at the edge of chaos: Phase transitions and emergent computation. *Physica D*. 1990;**42**:12–37.
- [21] Krawitz P. and Shmulevich I. Basin entropy in boolean network ensembles. *Physical Review Letters*. 2007;**98**:158701.
- [22] Lux T. and Marchesi M. Scaling and criticality in a stochastic multi-agent model of a financial market. *Nature*. 1999;**397**:498–500.
- [23] Prokopenko M., Boschetti F. and Ryan A. An information-theoretic primer on complexity, self-organization, and emergence. *Complexity*. 2009;**15**(1):11–28.
- [24] Crutchfield J. and Young K. *Computation at the onset of Chaos*. In: Zurek W. editor. *Entropy, Complexity, and the Physics of Information*. (Addison-Wesley: Massachusetts) 1990 p. 223–69.
- [25] Mitchell M., Hraber P. and Crutchfield J. Revisiting the edge of chaos: evolving cellular automata to perform computations. *Complex Systems* 1993;**7**:89–130.
- [26] Gencaga D., Knuth K. and Rossow W. A recipe for the estimation of information flow in a dynamical system. *Entropy*. 2015;**17**:438–70.
- [27] Schreiber T. Measuring information transfer. *Physical Review Letters* 2000;**85**:461–4.
- [28] Vicente R., Wibral M., Lindner M. and Gordon P. Transfer entropy—a model-free measure of effective connectivity for the neurosciences. *Journal of Computational Neuroscience*. 2011;**30**:45–67.
- [29] Lizier J. and Prokopenko M. Differentiating information transfer and causal effect. *The European Physical Journal B*. 2010;**73**:605–15.
- [30] Steeg G. and Galstyan A. Information transfer in social media. In: *21st World Wide Web Conference*. Lyon, France, April 16–20. ACM 2012.
- [31] Lizier J., Prokopenko M., and Zomaya A. Local measures of information storage in complex distributed computation. *Information Sciences* 2012;**208**:39–54.
- [32] Lizier J., Atay F. and Jost J. Information storage, loop motifs, and clustered structure in complex networks. *Physical Review E*. 2012;**86**:026110.
- [33] Faes L., Porta A., Rossato G., Adami A., Tonon D., Corica A. and Nollo G. Investigating the mechanisms of cardiovascular and cerebrovascular regulation in orthostatic syncope through an information decomposition strategy. *Autonomic Neuroscience*. 2013;**178**(1–2):76–82.
- [34] Wibral M., Lizier J., Vögler S., Priesemann V. and Galuske R. Local active information storage as a tool to understand distributed neural information processing. *Frontiers in Neuroinformatics* 2014;**8**(1):1–11.
- [35] Wang X., Miller J., Lizier J., Prokopenko M. and Rossi L. Quantifying and tracing information cascades in swarms. *PLoS ONE* 2012;**7**(7):e40084.
- [36] Cliff O., Lizier J., Wang X., Wang P., Obst O. and Prokopenko M. Quantifying long-range interactions and coherent structure in multi-agent dynamics. *Artificial Life*. 2017;**23**(1):34–57.
- [37] Crutchfield J. and Feldman D. Regularities unseen, randomness observed: levels of entropy convergence. *Chaos* 2003;**13**:25–54.
- [38] Vicious Syndicate Data Reaper Report. <https://www.vicioussyndicate.com/tag/data-reaper-report/>
- [39] Vicious Syndicate Data Reaper Report – FAQ. <https://www.vicioussyndicate.com/drr/faq-data-reaper-report/>
- [40] Shannon C. and Weaver W. *The Mathematical Theory of Communication*. (University of Illinois Press: Urbana-Champaign) 1949.
- [41] Feldman, D., McTague C. and Crutchfield P. The organization of intrinsic computation: Complexity-entropy diagrams and the diversity of natural information processing. *Chaos*. 2008;**18**(4):043106.
- [42] Prokopenko M., Lizier J., Obst O. and Wang X. Relating Fisher information to order parameters. *Physical Review E*. 2011;**84**:041116.
- [43] Hoffman R., Mueller S., Klein G. and Litman J. Metrics for explainable AI: Challenges and prospects. 2018; *arXiv preprint arXiv:1812.04608*.
- [44] Prokopenko M., Gerasimov V. and Tanev I. Measuring spatiotemporal coordination in a modular robotic system. In: Rocha L., Yaeger L., Bedau M., Floreano D., Goldstone R. and Vespignani A. (editors) *Artificial Life X: Proceedings of the 10th International Conference on the Simulation and Synthesis of Living Systems*. Bloomington IN, USA. MIT Press 2006 p. 185–91.
- [45] Arulkumar K., Cully A. and Togelius J. AlphaStar: An evolutionary computation perspective. In: *Proceedings of the Genetic and Evolutionary Computation Conference*. Prague, Czech Republic, July 13–17. ACM 2019 p. 314–5.
- [46] Gerlach M and Altmann E. Testing statistical laws in complex systems. *Physical Review Letters*. 2019;**122**(16):168301.
- [47] Zach T. Political events and the stock market: Evidence from Israel. *International Journal of Business*. 2003;**8**(3):243–66.
- [48] Dexter P. Historical analysis as a basis for population foresight. *Futures*. 2005;**38**:548–60.